Karyakos et al. *Iraqi Journal of Science, 2021, Vol. 62, No. 5, pp: 1537-1549*
DOI: 10.24996/ijs.2021.62.5.17

ISSN: 0067-2904

The dependence of spectral parameters in the cross-sectional equation of coherent and incoherent radiation on energy using a mathematical method

Raed Sabeeh Karyakos[1], Ilham M.Yacoob[2], Muna Y.Slewa[1],Amal M.Banoosh[2]

[1]Department of mathematics , college of Education , University of AL- Hamdaniya , Iraq

[2]Department of Physics , college of Education , University of AL –Hamdaniya

Received: 6/8/2020 Accepted: 23/10/2020

Abstract

The dependence of the cross-section of the coherent and incoherent radiation peaks in the X-ray absorption experiment of different energies (20-800 Kev) was investigated. Cross-sectional dependence on the atomic number Z was included from the published data for (8) elements, ranging from carbon to silver (C-Ag). The proportional constant K was obtained between (σ_c/σ_i), with the atomic number Z from (6-47). The results show that the value of K exponentially changes with energy.

Keywords: energy, mathematics, cross-sectional, X-ray, elements.

اعتماد المعاملات الطيفية في معادلة المقطع العرضي للأشعة المتشاكهة وغير المتشاكهة على الطاقة بطرق رياضية

رائد صبيح قرياقوس [1] ، الهام متي يعقوب[2] ، منى يوحنا صليوه[3] ، امل مجيد بنوش[4]

[1] كلية التربية، قسم الرياضيات ، جامعة الحمدانية

[2]كلية التربية، قسم الفيزياء ، جامعة الحمدانية

الخلاصه

اعتماد المقطع العرضي لقمم الاشعة المتشاكهة وغير المتشاكهة في تجربة امتصاص الاشعة السينية لمختلف الطاقات من (20-800) KeV . في هذا البحث تضمن اعتماد المقطع العرضي على العدد الذري Z من البيانات المنشورة لثمانية عناصر تتراوح من الكاربون الى الفضة (C-Ag) ، حيث تم الحصول على ثابت التناسب K من إجمالي المقطع العرضي الذري المتشاكة وغير المتشاكة (σ_c/σ_i) مع العدد الذري Z من (6-42) مبينا بان قيمة K تتغير اسيا مع الطاقة.

Introduction

Information on the constituents of trace elements in samples of biological, industrial, environmental, and geological origin is important for a variety of reasons. A number of analytical techniques are being used for this purpose. As compared to electron or charged particle excitation sources, X-ray excitation does not cause loss of volatile elements or other chemical changes. In X-ray fluorescence (XRF) analysis, the precise determination of trace element content in a specimen requires, among other factors, a correction factor that takes account of the absorption of primary and fluorescence X-ray in the specimen [1, 2]. Coherent and incoherent radiation scattering is a type of

*Email: Raed_sabeeh@yahoo.com

interaction of γ-rays and x-rays with matter. Coherent and Compton scattering are the basic processes for obtaining information about the structural properties of a substance. The coupled electrons of the atom, which dominate coherent scattering for most x-ray and low-energy γ modes, contribute to coherent scattering. In the physics of condensed matter, coherent and Compton scattering have also played a central role in understanding the excited states of many important systems [3, 4]. Coherent scattering of photons by atoms includes Rayleigh scattering, Thomson nuclear scattering, Delbrook scattering. and nuclear resonance scattering. Non-coherent scattering is one of the main processes by which γ-rays interact with a substance in the energy range from 0.1 to 5 MeV [2, 3,14]. Coherent and incoherent scattering sections are used in such diverse fields as medical X-ray technology, power reactor protection, industrial radiation treatment, and analysis of nuclear physics experiments (4).Van Espen *et al*. [5] used coherent to incoherent radiation scattering ratio to determine the effective sample weight. Van Dyck and Van Grieken [6 – 9] used absorption correction via scattered radiation in the energy dispersive X-ray fluorescence (EDXRF) analysis of samples of varying composition.Tursucu *et al*. [11] determined the effective atomic number of rare-earth
samples by using the scattering intensity ratio method. This ratio is used to determine the mean atomic number Z of the sample and expressed as the ratio of total coherent and incoherent atomic cross-section (σ_C/σ_i), with the following simple formula [10,12, 13]:

$$\sigma_C/\sigma_i = k Z^{(n-1)} \quad (1)$$

where K is an energy dependent constant according to Tomic et al [12], who used an M_o-tube coupled to an M_o foil and 90 detection angle, where (n-1) was found to be nearly 1.65. Since excitation energies are used nowadays in energy dispersed X-ray spectrometry, it is believed as desirable here to have a graph in which the variation of K and (n) parameters is displayed with the exciting radiation. It seems also desirable here to find out the explicitly that the cross- section of the coherent and non-coherent radiation peaks in the X-ray absorption experiment varies with Z for photon energies ranging from (20-800 Kev).

Theoretical Calculation

Values of the atomic cross-sections σ_c and σ_i are shown in Tables 1-13, taken from Hubbell *et al*. [11, 13] for the energies in the range of (20-800kev) which are supposed to strike the sample elements with an atomic number in the range of (6-47). Taking the natural logarithm, equation (1) may be written as:

$$Ln(\sigma_C/\sigma_i) = \ln K + (n-1) \ln \quad (2)$$

Table 1-Values of the atomic cross-sections σ_c and σ_i for an energy value of E=20kev [11, 13].

Z	ln *Z*	σ_c	σ_i	$\frac{\sigma_c}{\sigma_i}$	$\ln\frac{\sigma_c}{\sigma_i}$
6	1.7917	1.29	3.19	0.4044	-0.9054
13	2.5649	9.18	6.15	1.4927	0.4006
20	2.9957	25.5	8.82	2.8912	1.0617
26	3.258	48	10.8	4.4444	1.4917
29	3.367	64	11.6	5.5172	1.7079
35	3.555	102	13.2	7.7273	2.0448
42	3.737	158	15.2	10.3947	2.3413
47	3.85	209	16.9	12.5904	2.5329

Table 2-Values of the atomic cross-sections σ_c and σ_i for an energy value of E=40kev [11, 13].

Z	ln Z	σ_c	σ_i	$\frac{\sigma_c}{\sigma_i}$	ln $\frac{\sigma_c}{\sigma_I}$
6	1.7917	0.409	3.3	0.1239	-2.088
13	2.5649	3.08	6.7	0.4597	-0.7772
20	2.9957	8.66	9.87	0.8774	-0.1308
26	3.258	16.7	12.4	1.3468	0.2977
29	3.367	22.4	13.6	1.6471	0.499
35	3.555	36.7	15.9	2.3082	0.8365
42	3.737	57.8	18.5	3.1243	1.1392
47	3.85	76.3	20.3	3.7586	1.3241

Table 3-Values of the atomic cross-sections σ_c and σ_i for an energy value of E=60kev [11, 13].

Z	ln Z	σ_c	σ_i	$\frac{\sigma_c}{\sigma_I}$	ln $\frac{\sigma_c}{\sigma_I}$
6	1.7917	0.196	3.19	0.06144	-2.7897
13	2.5649	1.52	6.65	0.2286	-1.4759
20	2.9957	4.42	9.91	0.4460	-0.8047
26	3.258	8.51	12.6	0.6754	0.3925
29	3.367	11.4	13.9	0.8201	-0.1983
35	3.555	18.6	16.4	1.1341	0.1259
42	3.737	29.6	19.3	1.5337	0.4277
47	3.85	39.6	21.2	1.8679	0.6248

Table 4-Values of the atomic cross-sections σ_c and σ_i for an energy value of E=80kev [11, 13]

Z	ln Z	σ_c	σ_i	$\frac{\sigma_c}{\sigma_I}$	ln $\frac{\sigma_c}{\sigma_I}$
6	1.7917	0.114	3.05	0.03738	-32867
13	2.5649	0.898	6.45	01392	-1.9717
20	2.9957	2.64	9.69	0.2724	-1.3003
26	3.258	5.13	12.4	0.4137	-0.8826
29	3.367	6.86	13.7	0.5007	-0.6917
35	3.555	11.2	16.2	0.6914	-0.3691
42	3.737	17.8	19.2	0.9271	-0.0757
47	3.85	23.9	21.2	1.1274	0.1199

Table 5-Values of the atomic cross-sections σ_c and σ_i for an energy value of E=100kev [11, 13].

Z	ln *Z*	σ_c	σ_i	$\frac{\sigma_c}{\sigma_I}$	$\ln\frac{\sigma_c}{\sigma_I}$
6	**1.7917**	**0.0745**	**2.92**	**0.02551**	**-3.6685**
13	**2.5649**	**0.591**	**6.22**	**0.09502**	**-2.3537**
20	**2.9957**	**1.74**	**9.39**	**0.1853**	**-1.6858**
26	**3.258**	**3.37**	**12.0**	**0.2808**	**-1.2700**
29	**3.367**	**4.52**	**13.3**	**0.3398**	**-1.0793**
35	**3.555**	**7.39**	**15.9**	**0.4648**	**-0.7662**
42	**3.737**	**11.8**	**18.8**	**0.6277**	**-0.4658**
47	**3.85**	**15.8**	**20.9**	**0.7560**	**-0.2797**

Table 6-Values of the atomic cross-sections σ_c and σ_i for an energy value of E=150kev [11, 13].

Z	ln *Z*	σ_c	σ_i	$\frac{\sigma_c}{\sigma_I}$	$\ln\frac{\sigma_c}{\sigma_I}$
6	**1.7917**	**0.0339**	**2.65**	**0.01279**	**-4.3589**
13	**2.5649**	**0.276**	**5.68**	**0.04349**	**-3.1353**
20	**2.9957**	**0.810**	**8.64**	**0.09375**	**-2.3671**
26	**3.258**	**1.57**	**11.1**	**0.1414**	**-1.9559**
29	**3.367**	**2.10**	**12.4**	**0.1694**	**-1.7758**
35	**3.555**	**3.45**	**14.8**	**0.2331**	**-1.4563**
42	**3.737**	**5.53**	**17.7**	**0.3124**	**-1.1634**
47	**3.85**	**7.42**	**19.7**	**0.3766**	**-0.9764**

Table 7-Values of the atomic cross-sections σ_c and σ_i for an energy value of E=200kev [11, 13].

Z	ln *Z*	σ_c	σ_i	$\frac{\sigma_c}{\sigma_I}$	$\ln\frac{\sigma_c}{\sigma_I}$
6	**1.7917**	**0.0193**	**2.43**	**0.007942**	**-4.8355**
13	**2.5649**	**0.157**	**5.23**	**0.03002**	**-3.5059**
20	**2.9957**	**0.467**	**7.99**	**0.05845**	**-2.8396**
26	**3.258**	**0.907**	**10.3**	**0.08806**	**-2.4298**
29	**3.367**	**1.21**	**11.5**	**0.1052**	**-2.2517**
35	**3.555**	**1.99**	**13.8**	**0.1442**	**-1.9365**
42	**3.737**	**3.19**	**16.5**	**0.1933**	**-1.6433**
47	**3.85**	**4.28**	**18.4**	**0.2326**	**-0.4584**

Table 8 -Values of the atomic cross-sections σ_c and σ_i for an energy value of E=300kev [11, 13].

Z	ln Z	σ_C	σ_i	$\frac{\sigma_c}{\sigma_I}$	ln $\frac{\sigma_c}{\sigma_I}$
6	1.7917	0.00853	2.12	0.004024	-5.5156
13	2.5649	0.701	4.57	0.01534	-4.1773
20	2.9957	0.209	7.0	0.02986	-3.05113
26	3.258	0.407	9.08	0.04482	-3.1050
29	3.367	0.544	10.1	0.05386	-2.9213
35	3.555	0.892	12.2	0.07311	-2.6157
42	3.737	1.43	14.6	0.09795	-2.3233
47	3.85	1.93	16.3	0.1184	-2.1336

Table 9-Values of the atomic cross-sections σ_c and σ_i for an energy value of E=400kev [11, 13].

Z	ln Z	σ_c	σ_i	$\frac{\sigma_c}{\sigma_I}$	ln $\frac{\sigma_c}{\sigma_I}$
6	1.7917	0.00481	1.9	0.002532	-5.9789
13	2.5649	0.0396	4.1	0.009659	-4.6399
20	2.9957	0.118	6.3	0.01873	-3.9776
26	3.258	0.230	8.17	0.02815	-3.5701
29	3.367	0.308	9.10	0.03385	-3.3859
35	3.555	0.505	11.0	0.04591	-3.0811
42	3.737	0.812	13.1	0.06198	-2.7809
47	3.85	1.09	14.7	0.07415	-2.6017

Table 10- Values of the atomic cross-sections σ_c and σ_i for an energy value of E=500kev [11, 13].

Z	ln Z	σ_c	σ_i	$\frac{\sigma_c}{\sigma_I}$	ln $\frac{\sigma_c}{\sigma_I}$
6	1.7917	0.00308	1.73	0.0017803	-6.3309
13	2.5649	0.0255	3.75	0.0068	-4.9908
20	2.9957	0.0761	5.76	0.01321	-4.3266
26	3.258	0.148	7.47	0.01981	-3.9214
29	3.367	0.198	8.33	0.02377	-3.7394
35	3.555	0.324	10.0	0.0324	-3.4296
42	3.737	0.522	12.0	0.0435	-3.135
47	3.85	0.702	13.5	0.052	-2.9565

Table 11 -Values of the atomic cross-sections σ_c and σ_i for an energy level of E=600kev [11, 13].

Z	ln *Z*	σ_c	σ_i	$\frac{\sigma_c}{\sigma_I}$	$\ln\frac{\sigma_c}{\sigma_I}$
6	1.7917	0.00215	1.6	0.01344	-6.6123
13	2.5649	0.0177	3.47	0.005101	-5.2783
20	2.9957	0.0529	5.33	0.009925	-4.6127
26	3.258	0.103	6.92	0.01488	-4.2074
29	3.367	0.138	7.72	0.01788	-4.0243
35	3.555	0.225	9.31	0.02417	-3.7227
42	3.737	0.336	11.2	0.03241	-3.4293
47	3.85	0.488	12.5	0.0523904	-3.2432

Table 12-Values of the atomic cross-sections σ_c and σ_i for an energy value of E=800kev [11, 13].

Z	ln *Z*	σ_c	σ_i	$\frac{\sigma_c}{\sigma_I}$	$\ln\frac{\sigma_c}{\sigma_I}$
6	1.7917	0.00121	1.41	0.0008582	-7.0607
13	2.5649	0.00999	3.5	0.003275	-5.7213
20	2.9957	0.0298	4.69	0.006354	-5.0587
26	3.258	0.0580	6.09	0.009524	-4.6540
29	3.367	0.0776	6.79	0.01143	-4.4716
35	3.555	0.127	8.19	0.01551	-4.1665
42	3.737	0.204	9.82	0.02077	-3.8741
47	3.85	0.275	11.0	0.025	-3.6889

Results

Plots of $\ln(\sigma_c/\sigma_i)$ against lnz are shown in Figures (1-12) for photon energies of 20-800 keV, respectively, given as a straight line whose slope is (n-1) and y-intercept is (lnk) .This was performed for all the values of energies limited by the range of atomic number stated above.

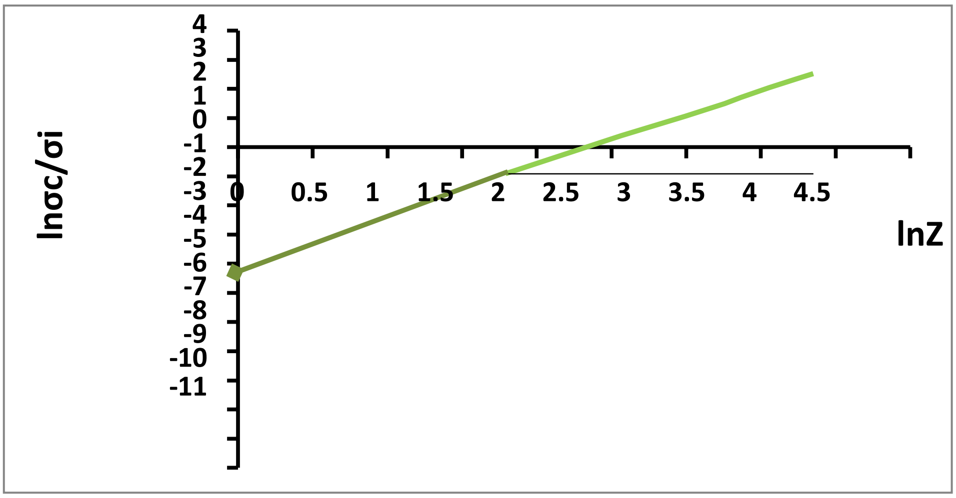

Figure 1- A plot of ln(σ_c/σ_i) against lnz for photon energy of 20 keV.

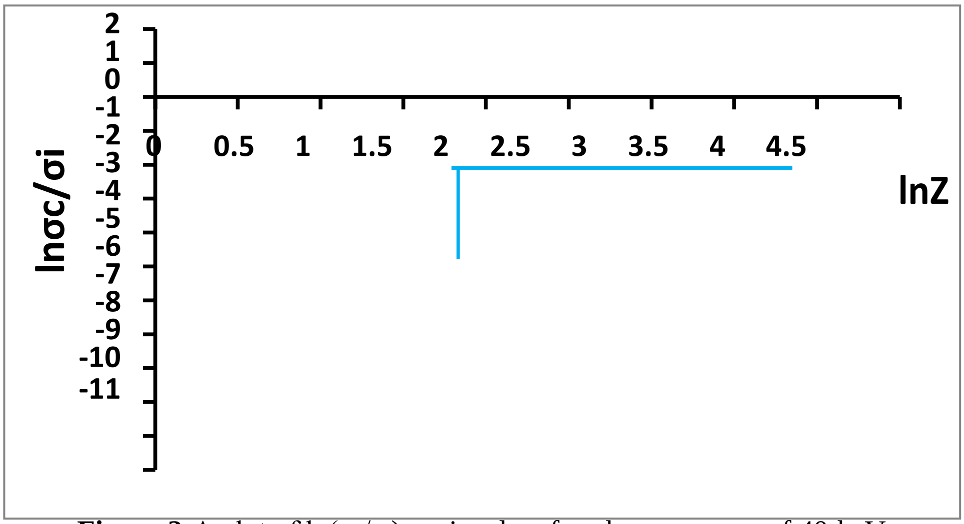

Figure 2-A plot of ln(σ_c/σ_i) against lnz for photon energy of 40 keV.

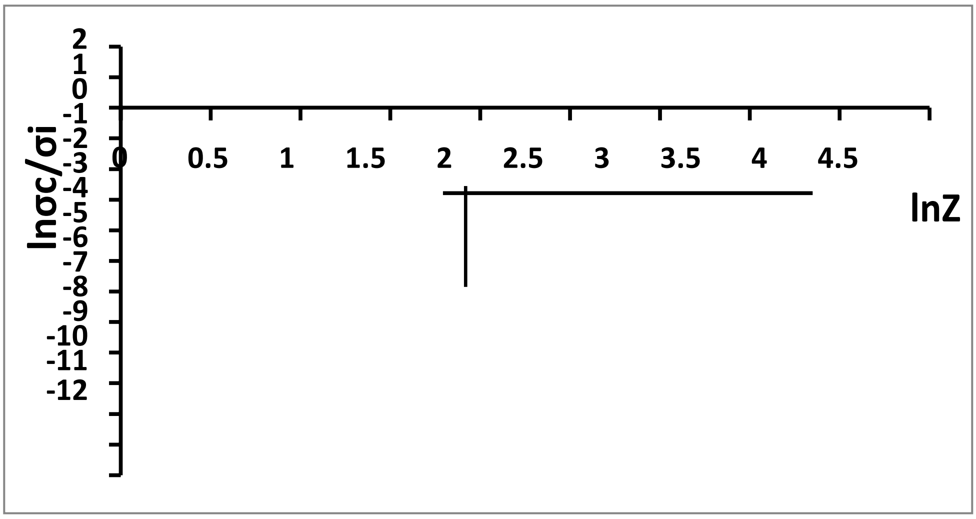

Figure 3-A plot of ln(σ_c/σ_i) against lnz for photon energy of 60 keV.

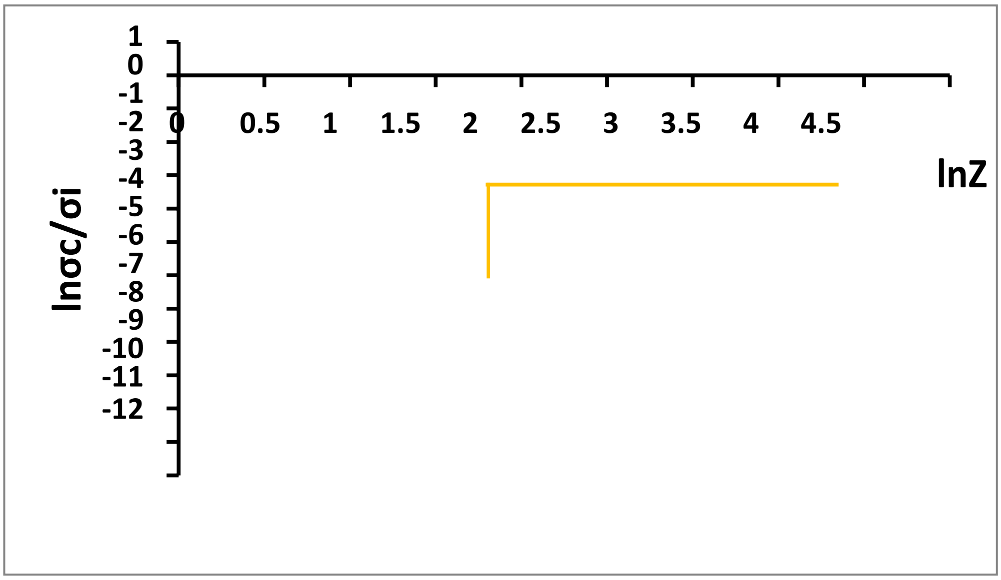

Figure 4-A plot of ln(σ_c/σ_i) against lnz for photon energy of 80 keV.

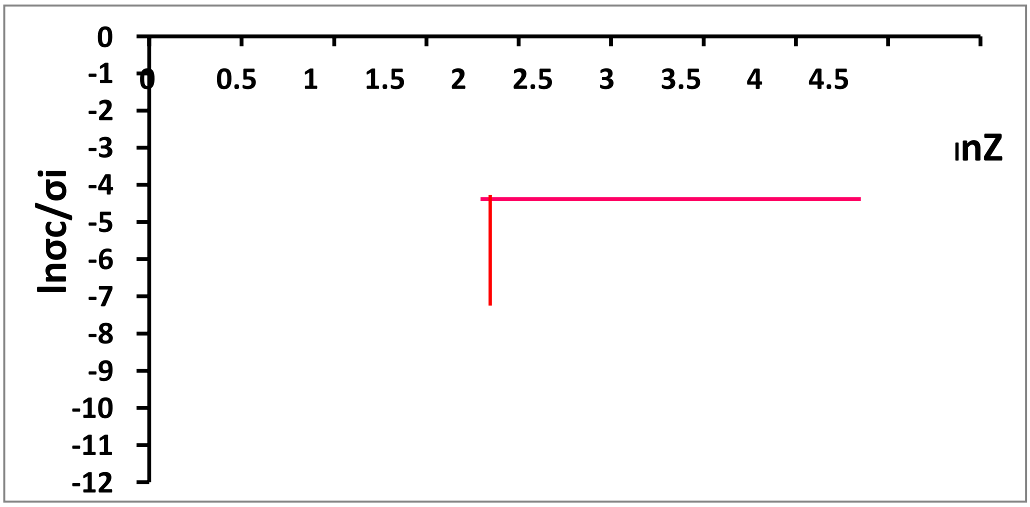

Figure 5-A plot of ln(σ_c/σ_i) against lnz for photon energy of 100 keV.

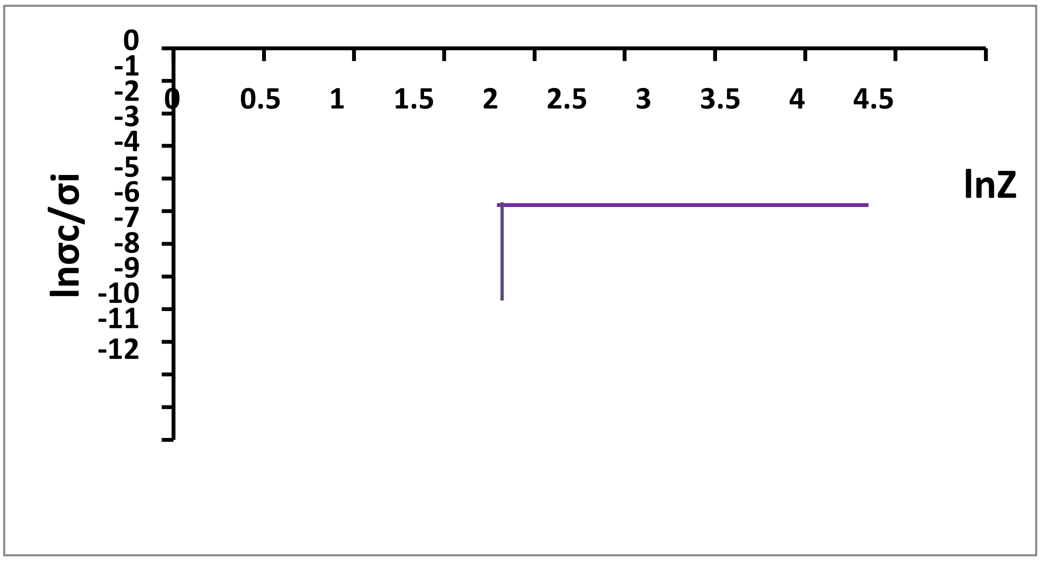

Figure 6-A plot of ln(σ_c/σ_i) against lnz for photon energy of 150 keV.

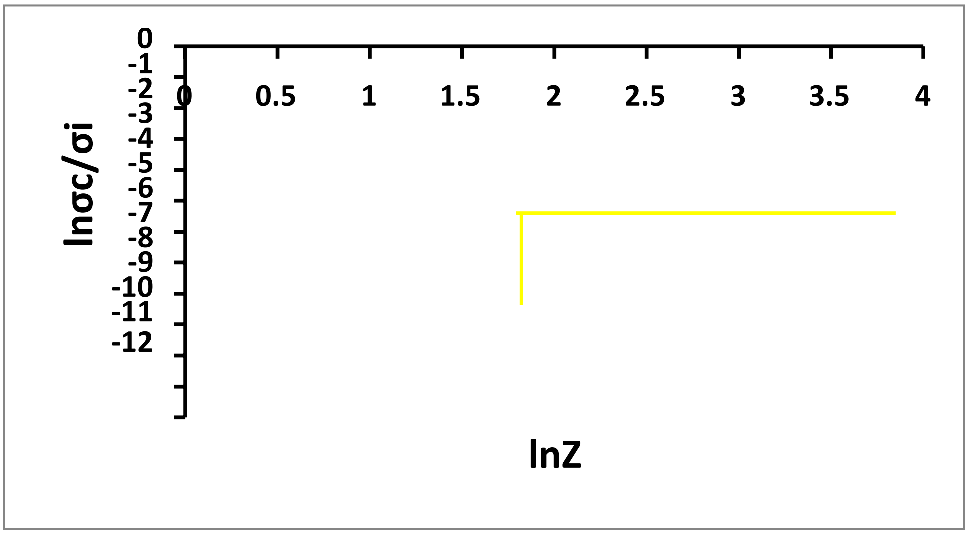

Figure 7-A plot of ln(σ_c/σ_i) against lnz for photon energy of 200 keV**.**

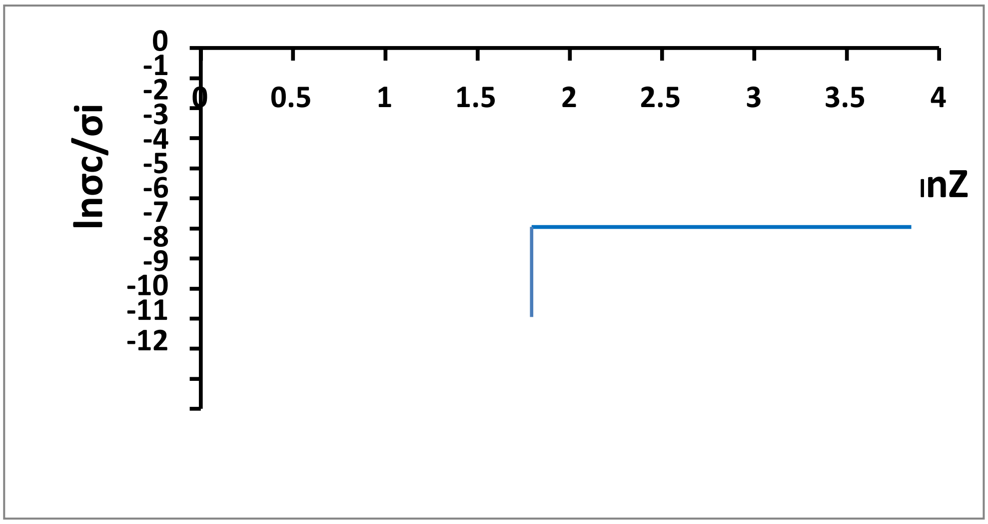

Figure 8-A plot of ln(σ_c/σ_i) against lnz for photon energy of 300 keV.

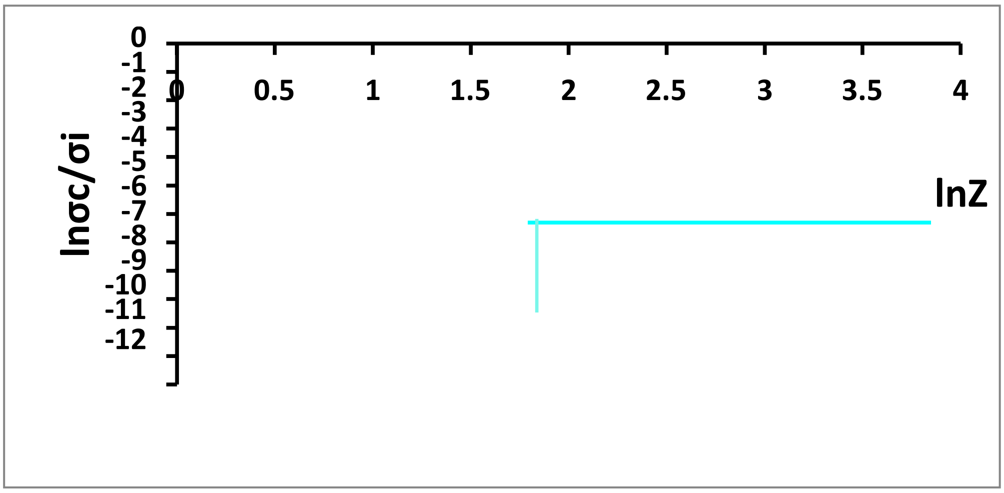

Figure 9-A plot of ln(σ_c/σ_i) against lnz for photon energy of 400 keV.

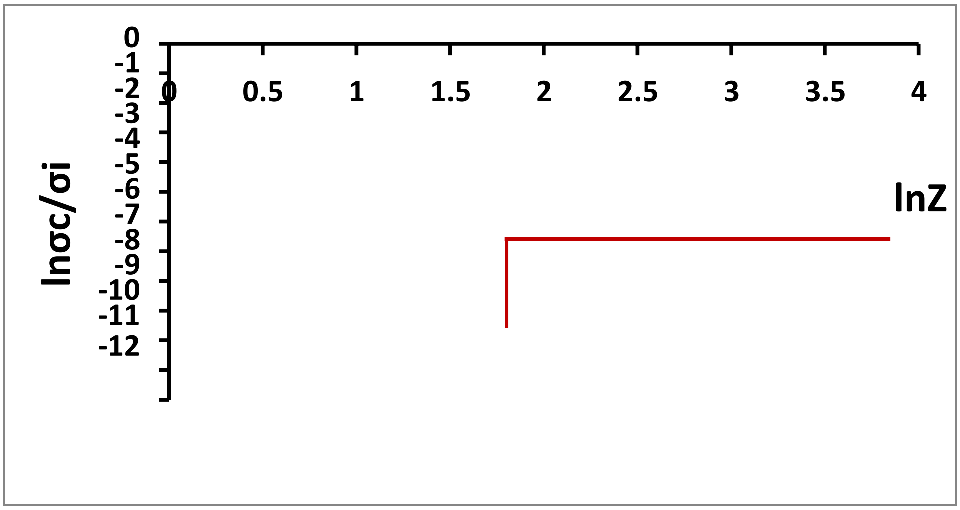

Figure 10-A plot of ln(σ_c/σ_i) against lnz for photon energy of 500 keV.

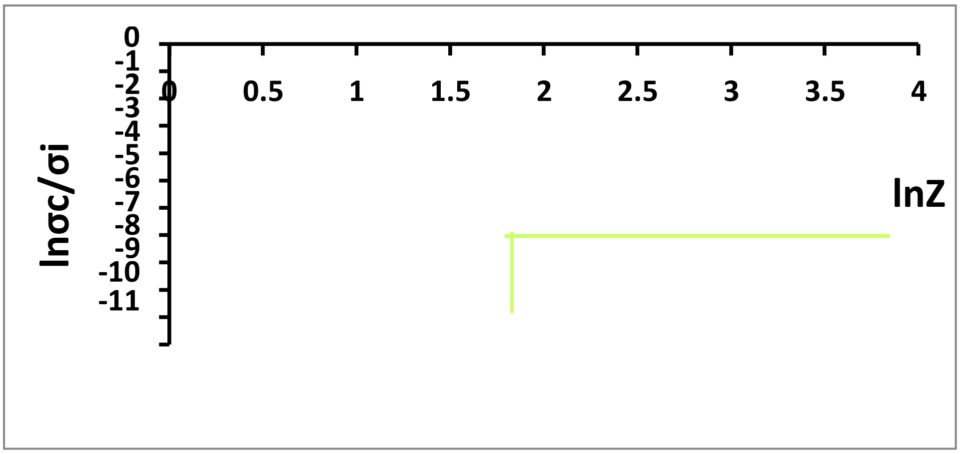

Figure 11- A plot of ln(σ_c/σ_i) against lnz for photon energy of 600 keV.

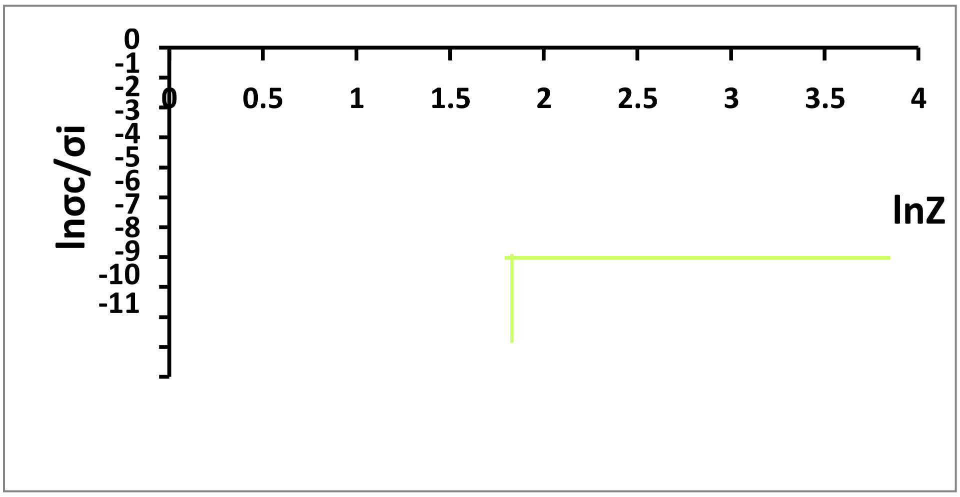

Figure 12-A plot of ln(σ_c/σ_i) against lnz for photon energy of 800 keV.

The energy dependent constant K was obtained using Microsoft Excel for tables (1-12) and graphs (1-12) for each of the different energy values (20-800 Kev). Table (13) and graph (13) which were obtained by using auto-cad program show the exponential change between the different energies with the energy dependent constant K .

Table 13-Values of different energy with the energy dependent constant K.

E(kev)	$slope = n - 1$	ln K	$K \times 10^{-4}$
20	1.6574	-3.878	206.92
40	1.645	-5.037	64.93
60	1.6433	-5.7268	32.6
80	1.6443	-6.222	19.85
100	1.6524	-6.6179	13.36
150	1.6512	-7.2983	6.767
200	1.6741	-7.73.85	4.528
300	1.6845	-8.516	2.00
400	1.6874	-8.98597.3	1.259
500	1.6904	-9.3493	0.8703
600	1.6924	-9.641	0.650
800	1.6943	-10.0905	0.415

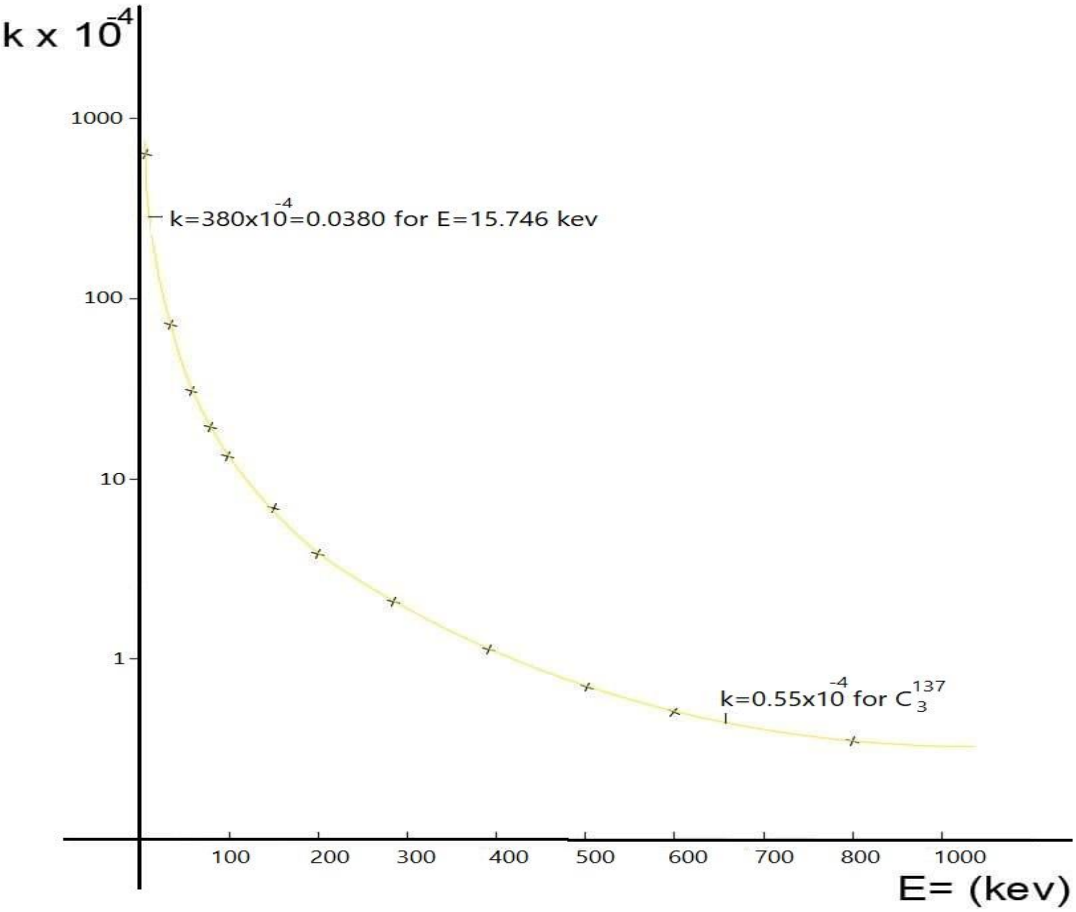

Figure 13-The relationship between the photon energies E and the energy dependent constant K.

Discussion and Conclusions

The dependence of the cross-section of the coherent and in-coherent radiation peaks in the x-ray absorption experiment of different energies (20-800 Kev) on the value of the atomic number was included based on the published data for (8) elements, ranging from (C-Ag). The obtained value of the energy dependent constant is not fixed for all elements, but rather changes exponentially with the value of photon energy . Therefore, we conclude that the energy dependent constant depends on the photon energies [14,15].

References

1. Prasad MN. Trace elements as contaminants and nutrients: consequences in ecosystems and human health.
2. John Wiley & Sons; 2008 Aug 20.
3. Brunetti A, Del Rio MS, Golosio B, Simionovici A, Somogyi A. A library for X-ray–matter interaction cross sections for X-ray fluorescence applications. Spectrochimica Acta Part B: Atomic Spectroscopy. 2004 Oct 8;59(10-11):1725-31.
4. Ridgers CP, Kirk JG, Duclous R, Blackburn TG, Brady CS, Bennett K, Arber TD, Bell AR. Modelling gamma-ray photon emission and pair production in high-intensity laser–matter interactions. Journal of computational physics. 2014 Mar 1;260:273-85.
5. Çatal N, Ertuğrul M, Özdemir Y. Investigation of coherent to incoherent scattering cross section ratios of some foil metals depending on the temperature. InJournal of Physics: Conference Series 2016 Apr (Vol. 707, No. 1, p. 012007). IOP Publishing.
6. Van Espen P, Van't Dack L, Adams F, Van Grieken R. Effective sample weight from scatter peaks in energy-dispersive X-ray fluorescence. Analytical Chemistry. 1979 Jun 1;51(7):961-7.

7. Van Dyck PM, Van Grieken RE. Absorption correction via scattered radiation in energy-dispersive X-ray fluorescence analysis for samples of variable composition and thickness. Analytical chemistry. 1980 Oct 1;52(12):1859-64.

8. A.D. Pogrebnjak, A.A. Muhammed, E.T. Karash, N.Y. Jamil, J. Partyka, Przegląd Elektrotech. 89, 315 (2013).

9. A. D. Pogrebnyak, A. M. Mahmud, E. T. Karasha, G. V. Kirik, R. Y. Tkachenko and A. P. Sypylenko, "Structure and Physical-Mechanical Properties of Nc-TiN Coatings Obtained by Vacuum-Arc Deposition and Deposition of HF Discharge," Journal of Nano- and Electronic Physics, Vol. 3, No. 4, 2011, pp. 97-105.

10. A. D. Pogrebnyak, A. M. Mahmud, E. T. Karasha, " Structural properties of nanocrystalline tin film," International Journal Of Structronics & Mechatronics, May 27, 2012.

11. Abdullah AN. Elastic electron scattering from 6He and 11Li halo nuclei. Iraqi Journal of Science. 2018;59(2C):1057-64.

12. Turşucu A, Demir D, Önder P. Effective atomic number determination of rare earth oxides with scattering intensity ratio. Science and Technology of Nuclear Installations,2013.

13. Hubbell JH. Review and history of photon cross section calculations. Physics in Medicine & Biology. 2006 Jun 20;51(13):R245.

14. Tomic S.,Krmpotic-Nemanic J. and Valkovic V. X-ray fluorescence of (irregularly shaped)bon samples material,nuclear instruments and methods in physics research,198;818,pp7176.

15. Noori RI, Ridha AR. Density Distributions and Elastic Electron Scattering Form Factors of Proton-rich 8B, 17F, 17Ne, 23Al and 27P Nuclei. Iraqi Journal of Science. 2019 Jun 26:1286-96.

16. Radon Concentration Measurement in Ainkawa Region Using Solid State Nuclear Track Detector Hanaa N. Azeez, Malik H. Kheder, Muna Y. Slewa, Sleeman Y. Sleeman